PLANT SCIENCE TODAY
Vol x(x): xx–xx
https://doi.org/10.14719/pst.11922

eISSN 2348-1900

RESEARCH ARTICLE

# Exploring the anticancer potential of bioactive fractions of *Erythrina variegata* L. in MDA-MB-231 cell lines

**Parvathy V & Bibu John Kariyil***

Department of Veterinary Pharmacology and Toxicology, College of Veterinary and Animal Sciences, Kerala Veterinary and Animal Sciences University, Mannuthy, Thrissur 680 651, Kerala, India

*Correspondence email - bibujohn@kvasu.ac.in

Received: 23 September 2025; Accepted: 23 December 2025; Available online: Version 1.0: 31 March 2025

**Cite this article:** Parvathy V, Bibu JK . Exploring the anticancer potential of bioactive fractions of *Erythrina variegata* L. in MDA-MB-231 cell lines. Plant Science Today (Early Access). https://doi.org/10.14719/pst.11922

## Abstract

*Erythrina variegata* L. (Fabaceae) has been traditionally reported to possess antitumour, expectorant, febrifuge, antibacterial and antioxidant properties. In the present work, the methanol extract of stem bark of *E. variegata* (MEV) and its fractions such as hexane (HFEV), chloroform (CFEV), ethylacetate (EAFEV) and methanol (MFEV) were assessed for their cytotoxic potential against triple-negative breast cancer (TNBC) cell line MDA-MB-231 using the 3-(4,5-dimethylthiazol-2-yl)-2,5-diphenyl tetrazolium bromide (MTT) assay. In this MTT assay, the chloroform fraction was found to be the most potent. Apoptotic changes induced by CFEV were further examined through acridine orange/ethidium bromide (AO/EB) dual staining and 4′, 6-diamidino-2-phenylindole (DAPI) staining. Expression of the antiapoptotic gene *Bcl-2* was analysed by real-time polymerase chain reaction (RT-PCR). Phytochemical profiling of the extract was carried out by gas chromatography-mass spectrometry (GC-MS) and high resolution liquid chromatography mass spectrometry (HRLC-MS). The findings demonstrated a concentration -dependent cytotoxic effect of CFEV in the cell lines. In silico docking study revealed that compounds like melochinone (-8.4 kcal/mol), sesamin (-7.9 kcal/mol), muricinine (-7 kcal/mol), 5-hydroxy-3-methoxysativan (-7.3 kcal/mol), 2,3-dihydroxy p-cumate (-6.2 kcal/mol) and alpinumisoflavone (-8.3 kcal/mol) had good binding affinity with *Bcl-2* protein. Furthermore, it triggered apoptotic cell death through the mitochondrial-dependent intrinsic pathway, suggesting that *E. variegata* may serve as a promising source of bioactive compounds with therapeutic potential against breast cancer.

**Keywords:** AO/EB staining; DAPI staining; *Erythrina variegata*; GC-MS; HRLC-MS; *in silico* docking; MDA-MB-231 cell line; molecular study

## Introduction

Breast cancer is the most common malignancy affecting the female population. Among its subtypes, triple-negative breast cancer (TNBC) is a heterogeneous disease characterized by different clinical, pathological and biological features, representing approximately 10 to 20 % of all breast cancer cases globally, with higher prevalence observed among black women and younger populations (1). It possess a major challenge in its treatment due to the lack of hormone receptors. The absence of these receptors makes hormone therapy and HER2-directed treatments ineffective, leaving patients dependent on non-specific options like surgery and chemotherapy. TNBC is often linked to early metastasis, frequent recurrence and poor overall prognosis, especially among younger, premenopausal women (2). Genetic alterations, particularly mutations in the breast cancer susceptibility gene 1 (BRCA1), are key drivers in TNBC development, as they disrupt DNA repair mechanisms and enhance genomic instability (3). Conventional therapy is often associated with side effects and has limited therapeutic success in advanced stages of cancer. Therefore, the search for new therapeutic agents from plant sources may provide an alternative cancer treatment. Phytocompounds isolated from plants have been reported to have anticancer activity *in vitro* including alkaloids, phenolics, flavonoids, quinones, coumarins, lignans, stilbenes and tannins (4).

The genus *Erythrina* (Fabaceae) comprises more than 100 species distributed across tropical and subtropical regions worldwide. *E. variegata*, a tall ornamental tree found throughout the upper Gangetic plains of India and Nepal, has long been valued for its medicinal properties. In Chinese herbal medicine, it is employed for the treatment of pyrexia, scabies and septicemia due to its antibacterial and anti-inflammatory activities. Traditionally, the bark is regarded as astringent, febrifuge, anti-bilious and anthelmintic, and is used in the management of ophthalmic and dermatological conditions. The leaves are applied in the treatment of fever, inflammation and joint pain, while the leaf juice is used to alleviate earache and toothache (5). The roots possess febrifuge, bronchodilatory and insecticidal properties and are also reported to be effective in treating cancer, convulsions and skin ailments such as pimples (6). Furthermore, the plant has been used as a laxative, diuretic and expectorant (7). The stem bark of *E. variegata* contains flavonoids, alkaloids and phenolic compounds, which have demonstrated potential cytotoxic and apoptotic activity in Michigan Cancer Foundation (MCF)-7 and M.D. Anderson-mammary/breast-231 (MDA-MB-231) cell lines (8). However, the specific bioactive fractions responsible for these effects on TNBC cells remain largely uninvestigated.

The present study aims to address this research gap by investigating the anticancer potential of bioactive fractions derived from the methanolic extract of *E. variegata* against the MDA-MB-231 cell line, a well-established model of TNBC. In addition, the study seeks to elucidate the molecular mechanisms by which these bioactive fractions mediate their anticancer activity.

## Materials and Methods

### Chemicals and drugs

Deoxyribonucleic acid (DNA) ladder (100 bp); 3-(4, 5-dimethylthiazol-2-yl)-2, 5- diphenyltetrazolium bromide (MTT); Acridine Orange hemi (zinc chloride) salt; Agarose; Antibiotic-antimycotic solution (100X); Blue/orange 6X gel loading dye; Ceftriaxone; Chloroform (99–99.4 %); Cisplatin; Boric acid (99.50 %); Dimethylsulphoxide (DMSO); Disodium ethylenediaminetetraacetic acid; Dulbecco's Phosphate-buffer; Ethidium bromide; Foetal bovine serum (FBS); GT PCR master mix (EmeraldAmp® GT PCR Master mix, TaKaRa); Isopropanol (99 %); GoTaq® qPCR master mix; Methanol; Nuclease-free water; Nucleotide primers for GAPDH and Bcl-2; Leibovits-15; TRI Reagent; Tris (hydroxymethyl) aminomethane, Tromethamine (Tris base); Trypan blue stain 0.4 %; Trypsin (0.25 %)-EDTA (IX) ; Verso cDNA synthesis kit .

### Collection of plant material and authentication

The stem bark of *E. variegata* was collected from the Palakkad and Idukki district, Kerala. The bark was sampled in June and July 2024. The plant material was molecularly authenticated by Rajiv Gandhi Centre for Biotechnology, Poojapura, Thiruvananthapuram and the voucher specimen has been deposited in the Department of Veterinary Pharmacology and Toxicology, College of Veterinary and Animal Sciences, Mannuthy, with accession no. HERB/VPT/CVASMTY/2/2024.

### Methanol extraction

The stem bark of *E. variegata* (1 kg) was shade dried at room temperature and coarsely powdered using an electric pulverizer. The powder obtained (870 g) was extracted by continuous hot reflux method with methanol (99 % v/v) at 67 °C. The methanol extract thus obtained was then concentrated in the rotary vacuum evaporator under reduced pressure and temperature (40 °C) and kept under refrigeration after complete evaporation of the solvent in an airtight container.

### Preparation of different fractions of crude methanol extract of *Erythrina variegata* (MEV)

One gram of MEV of *E. variegata* was sequentially fractionated with solvents of increasing polarity. The extract was first dissolved in water and partitioned with hexane to obtain the hexane fraction (HFEV). The aqueous residue was subsequently extracted with chloroform, ethyl acetate and methanol to yield the chloroform (CFEV), ethyl acetate (EAFEV) and methanol (MFEV) fractions respectively, while the remaining aqueous phase was collected as the water fraction. All fractions were concentrated using a rotary vacuum evaporator and stored under refrigeration until further use.

### Sample preparation

The crude methanol extract and its fractions were solubilized in dimethyl sulphoxide (DMSO) at a concentration of 5.0 mg/mL, further, this stock solution was diluted with complete Leibovitz's (1X) L-15 medium to required concentrations. The final concentration of DMSO in the well was maintained at less than 1 % w/v.

### Culturing of cell lines

MDA-MB-231 line was procured from the Cell Repository, National Centre for Cell Sciences, Pune, India. The cells were cultured in Leibovitz's (1X) L-15 medium supplemented with 10 % foetal bovine serum and 4 % antibiotic-antimycotic solution containing penicillin-streptomycin and amphotericin B. The cells were maintained in a humidified incubator at 37 °C. The cells were sub-cultured by enzymatic digestion with 0.25 % trypsin and 1 mM ethylene diamine tetraacetic acid solution after attaining 70 % confluency. Trypsinized cells were used for MTT assay.

### *In vitro* cytotoxic study of MEV and their fractions

The MTT assay was done to assess the cytotoxicity of MEV and its fractions as per the method of (9). The MDA-MB-231 breast cancer cell lines were seeded at a density of $10\times10^3$ cells per well in 200 µL medium and were allowed to attach overnight in a $CO_2$ incubator. Cells were treated with methanol extract and their fractions- HFEV, CFEV, MFEV, EAFEV separately at concentrations of 10, 20, 40, 80 and 160 µg/mL respectively, for a period of 48 hr. After the treatment, 10 µL of MTT (3 mg/mL) in 100 µL medium was added and incubated at 37 °C for 4 hr after removing the medium with crude extract and its fractions of *E. variegata*. Then the medium with MTT was removed and the formed purple formazan crystals were dissolved in 200 µL of DMSO and read at 570 nm in an ELISA plate reader (Varioskan Flash, Thermo Fischer Scientific, Finland). The per cent cell viability was calculated using the formula:

Per cent cell viability = (Average absorbance of treated cells/ Average absorbance of untreated cells) × 100.

The half maximal inhibitory concentration ($IC_{50}$) values for the treatments were calculated using GraphPad Prism version 5.00 (GraphPad Software, San Diego, California USA).

### Assessment of apoptotic changes

#### Microscopic study using acridine orange/ethidium bromide (AO/EB) staining

The AO/EB staining procedure was followed to differentiate the live, apoptotic and necrotic cells. Cells with a seeding density of $1x10^5$ cells/well were seeded into a 6 well plate and allowed to grow for 24 hr. Then, the cells were treated with the $IC_{50}$ concentration of CFEV and cisplatin for 24 hr, with one well left as the negative control. Acridine orange and ethidium bromide stock solutions were prepared by dissolving 10 mg of the dye powders in 1 mL of phosphate buffered saline (PBS) each separately. The working dual AO/EB stain solution was prepared by adding 1 µL of both stain stock solutions to 98 µL of PBS. After 24 hr, the spent medium was removed and the cells were fixed with paraformaldehyde solution for 10–20 min. Then the solution was removed and 500 µL of AO/EB stain was added to each well and examined under a trinocular research fluorescence microscope, DM 2000 LED, Leica with blue excitation (488 nm) and emission (550 nm) filters at 20x magnification (10).

#### Analysis of morphological changes in nucleus

Cells with a seed density of $1x10^5$ cells/well were seeded into a six well plate and allowed to grow for 24 hr. Then, the cells were treated with the $IC_{50}$ concentration of CFEV and cisplatin for 24 hr, with one well left as the negative control. The DAPI stock solution was prepared by dissolving 1 mg of dye powder in 1 mL of PBS. The working solution was prepared by adding 1 µL of stock solution to

99 µL of PBS. After 24 hr, the spent medium was removed and the cells were fixed with paraformaldehyde solution for 10–20 min. Then the solution was removed and 500 µL of DAPI stain was added to each well and examined under a trinocular research fluorescence microscope, DM 2000 LED, Leica with blue excitation (359 nm) and emission (461 nm) filters at 20x magnification.

**Gene expression study**

The reverse transcription quantitative polymerase chain reaction (RT-qPCR) technique was used for studying the gene expression of the *Bcl-2* gene in cell culture samples. Briefly, the cells were treated with the potent fraction at its $IC_{50}$ concentration for 24 hr. RNA was obtained from control and fraction-treated cells by the conventional TRI reagent method. From the obtained RNA, complementary DNA (cDNA) synthesis was carried out from total RNA (500 ng) using the verso cDNA Synthesis Kit (Thermoscientific, USA) as per the manufacturer's protocol. The reaction mixture was then subjected to PCR for amplification of the *Bcl-2* gene using specifically designed primers by Primer3 an online primer design software (Primer3, http://bioinfo.ut.ee/primer3/). *Bcl-2* primer (*Bcl-2* Forward: 5' TGGATCCAGGATAACGGAGG-3'; *Bcl-2* Reverse: 5' CAAACAGAGGTCGCATGCTG-3)'. The housekeeping gene GAPDH (Forward: 5'-CAACGAATTTGGCTACAGCA-3'; Reverse: 5'-AGGGGAGATTCAGTGTGGTG-3') was co-amplified in each reaction as an internal control. The RT-qPCR was carried out in a final volume of 10 µL containing 250 ng of template cDNA, GoTaq® qPCR mastermix (5 µL) and 10 pM/µL of each primer. In the negative control, template cDNA was replaced with NFW water. Separate PCR reactions were performed for the target gene (*Bcl-2*) and the reference housekeeping gene (GAPDH). Each reaction was carried out in triplicate in a 10 µL volume. The thermal cycling conditions included an initial denaturation at 95 °C for 5 min, followed by 40 amplification cycles consisting of denaturation at 95 °C, annealing at 61 °C for *Bcl-2* and 56.1 °C for GAPDH for 30 sec, and extension at 72 °C for 35 sec. A final extension step was performed at 72 °C for 1 min. Relative expression of the *Bcl-2* gene was determined using the comparative $C_T$ ($\Delta\Delta C_T$) method and presented as the fold change (up-regulation or down-regulation) in transcript levels compared with the untreated control group (11).

Fold change = $2^{-\Delta\Delta C_T}$, where $\Delta\Delta C_T$ = ($C_T$ target gene - $C_T$ GAPDH) treated - ($C_T$ target gene - $C_T$, GAPDH) control.

## Phytochemical screening

The chloroform fraction of *E. variegata* was subjected to preliminary phytochemical screening to identify the major classes of phytoconstituents present (12).

## Gas chromatography mass spectrometry (GC-MS) analysis

The active phytochemical principles of CEFV were analysed using the GC-MS system at the Centre for Analytical Instrumentation-Kerala (CAI-K), Kerala Forest Research Institute (KFRI), Peechi, Kerala. Gas chromatography mass spectrometer (Shimadzu GC-MS, Japan, QP2010S) with a mass range of 1.5–1000 m/z was used. Helium was used as the carrier gas at a flow rate of 1 mL/min. The oven temperature was maintained at 80 °C for 4 min and then increased to 280 °C in 6 min. The injector temperature was 260 °C and the total analysis time was 50 min. Aliquots of extracts (0.4 µL) were injected into the chromatographic column after a clear baseline was obtained (13). Major constituents were identified by using mass spectrum libraries (NIST 11 and WILEY 8).

## High-resolution liquid chromatography mass spectrometry (HR-LCMS) analysis

High-resolution liquid chromatography mass spectrometry analysis of CFEV was carried out at the Indian Institute of Technology (IIT), Bombay, using an Agilent LC-QTOF-MS system. The setup included a binary pump (G220B), a HiP auto sampler (G4226A) and a column compartment (G1316C) maintained at 40 °C. A 5 µL sample was injected with a flow rate of 0.3 µL/min. Chromatographic separation was achieved using a mobile phase of water with 0.1% formic acid (A) and acetonitrile (B), following a linear gradient (5 % to 100 % B over 25 min, returning to 5 % by 35 min). Detection was performed with a QTOF mass spectrometer coupled with a diode array detector (G226A), using dual ESI in both positive and negative modes (m/z range: 120–1200; scan rate: 100 spectra/sec). Ion source parameters included a drying gas temperature of 250 °C, gas flow of 13 L/min, nebulizer at 35 psig, and capillary voltage of 3500 V. Data were processed using Agilent Mass Hunter software for constituent identification and the mass-to-charge (m/z) analysis based on accurate mass and fragmentation data.

## *In silico* analysis of phytocompounds

Phytochemicals identified from GC-MS and HR-LCMS were screened for biological activity using the PASS server (14) and compounds with predicted antineoplastic activity were further evaluated for drug -likeness and Lipinski's rule violation, with the help of the software Swiss ADME (http://www.swissadme.ch). The 3D structure of human Bcl-2 (PDB ID: 4LXD) was retrieved from the RCSB Protein Data Bank and prepared using Discovery Studio Visualizer 3.5 and AutoDock Tools (v1.5.6). Ligand structures were obtained from the PubChem database in SDF format, optimized in ADT and converted to PDBQT files. Molecular docking was carried out in AutoDock 4 using the Lamarckian genetic algorithm with a grid size of 40 × 40 × 40 (spacing 1 Å, grid center: x = 24.2, y = 32.6, z = 10.05). Binding interactions and hydrogen bonds were visualized with Discovery Studio Visualizer (v16.1.0.15350) and binding energies (kcal/mol) were obtained from the docking log files.

## Statistical analysis

All results were expressed as mean ± SE with 'n' equal to the number of replicates. The $IC_{50}$ values of various treatments were calculated using the GraphPad Prism version 5. All the statistical analysis was conducted using IBM SPSS Statistics for Windows, version 21 (IBM Corp., Armonk, NY, USA). Two-way analysis of variance (ANOVA) followed by the LSD post hoc test was used to compare the significant differences among and within various treatments on percent cell inhibition. One-way ANOVA followed by Tukey's multiple comparison test was used to compare the significant differences among various treatments on relative gene expression.

# Results

The shade-dried bark of *E. variegata* was molecularly authenticated at the Rajiv Gandhi Centre for Biotechnology, Thiruvananthapuram, Kerala. On BLAST analysis it was found that the amplified forward and reverse sequences had 99 % and 99.63 % similarity respectively, with the *rbcL* gene, confirming high sequence homology.

The yield of crude methanol extract of the bark of *E. variegata* was found to be 5 % with respect to its initial dry weight (80 g). The yield of different fractions of MEV was presented in Table 1. The yields of respective fractions were calculated on the basis of initial

**Table 1.** Yield of different fractions of methanolic crude extract of *Erythrina variegata* (MEV)

| Sl. No. | Fractions | Weight of crude extract (mg) | Obtained fraction weight (mg) | Extraction yield (%) |
|---|---|---|---|---|
| 1 | HFEV (Hexane fraction) | 500 | 82 | 16.4 |
| 2 | CFEV (Chloroform fraction) | 500 | 214 | 42.8 |
| 3 | EAFEV (Ethyl acetate fraction) | 500 | 53.4 | 10.68 |
| 4 | MFEV (Methanol fraction) | 500 | 117.6 | 23.52 |
| 5 | WFEV (Aqueous fraction) | 500 | 0 | 0 |

dry weight (500 mg) of methanol extract of respective plants.

The cytotoxic potential of the methanolic extract of *E. variegata* (MEV) and its solvent fractions (HFEV, CFEV, EAFEV, and MFEV) was evaluated in MDA-MB-231 cells using the MTT assay. The data of MTT reduction assay was depicted in Table 2 and Fig. 1. All extracts exhibited a concentration-dependent inhibition of cell viability, with maximum cytotoxicity observed at 160 µg/mL. Among the fractions, the chloroform fraction (CFEV) showed the most potent activity, with inhibition comparable to cisplatin ($p < 0.001$). The $IC_{50}$ values were calculated as 20.43 ± 1.15 µg/mL (MEV), 32.33 ± 1.18 µg/mL (HFEV), 19.01 ± 1.37 µg/mL (CFEV), 26.68 ± 1.12 µg/mL (EAFEV) and 26.40 ± 1.20 µg/mL (MFEV), compared with 20.71 ± 0.96 µg/mL for cisplatin. These results indicated that the CFEV fraction is the most active constituent of *E. variegata*, exerting cytotoxic effects comparable to the standard drug.

In AO/EB staining, the control cells showed uniform green fluorescence with centrally located, intact nuclei (Fig. 2A). Fig. 2B and Fig. 2C depicted representative images of treated cells after AO/EB staining. Treated cells displayed at its $IC_{50}$ concentrations predominantly orange-stained nuclei, indicative of apoptosis, along with the presence of a few necrotic cells.

The apoptotic changes in the MDA-MB-231 cell lines treated with $IC_{50}$ concentrations of CFEV and cisplatin are shown in Fig. 3. The control cell emitted blue fluorescence, indicating live cells whereas treated cells showed bright blue fluorescence which indicated the apoptotic change ie., fragment of nucleic acid.

The relative *Bcl-2* gene expression in the MDA-MB-231 cell line in response to addition of CFEV at its $IC_{50}$ concentration as compared with control is presented in Table 3. In MDA-MB-231 cells, *Bcl-2* gene expression was decreased significantly ($p < 0.01$) for the chloroform

**Table 2.** Cytotoxic studies of crude extract and their fractions of *Erythrina variegata* and cisplatin with various concentrations

| Treatment | Concentrations (µg/mL) | | | | |
|---|---|---|---|---|---|
| | 10 | 20 | 40 | 80 | 160 |
| MEV | $15.48^{cD} \pm 1.08$ | $48.23^{bcC} \pm 1.02$ | $83.5^{aB} \pm 0.94$ | $95.73^{aA} \pm 1.37$ | $95.6^{aA} \pm 1.01$ |
| HFEV | $22.32^{bD} \pm 1.07$ | $31.51^{dC} \pm 1.50$ | $55.82^{cB} \pm 1.70$ | $78.75^{cA} \pm 2.10$ | $83.00^{aA} \pm 3.88$ |
| CFEV | $28.97^{aE} \pm 2.9$ | $55.35^{aD} \pm 2.38$ | $69.24^{bC} \pm 2.81$ | $83.37^{bcB} \pm 3.75$ | $98.66^{aA} \pm 0.49$ |
| EAFEV | $25.64^{abE} \pm 0.93$ | $43.36^{cD} \pm 0.75$ | $70.55^{bC} \pm 2.26$ | $77.94^{cB} \pm 2.67$ | $87.09^{aA} \pm 1.87$ |
| MFEV | $26.11^{abD} \pm 2.24$ | $42.68^{cC} \pm 1.17$ | $60.78^{cB} \pm 3.91$ | $63.81^{dB} \pm 3.11$ | $99.66^{aA} \pm 0.21$ |
| Cisplatin | $15.76^{cE} \pm 0.39$ | $51.47^{abD} \pm 1.24$ | $68.12^{bC} \pm 1.37$ | $89.00^{bB} \pm 2.04$ | $97.53^{aA} \pm 0.75$ |

** Significant at 0.01 level; *Means having different small letter as superscript differ significantly within a column; *Means having different capital letter as superscript differ significantly within a raw

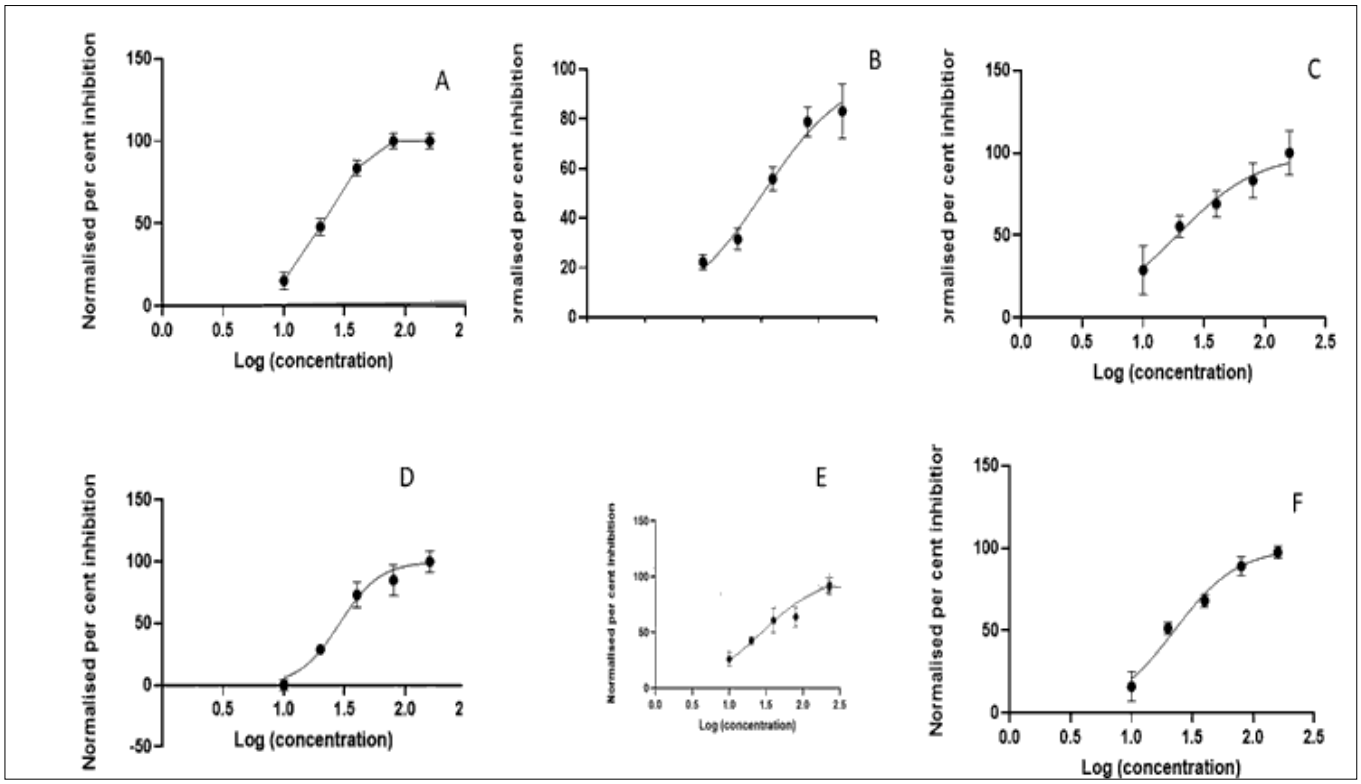


**Fig. 1.** Dose response curve of percent of inhibition of crude extract of *Erythrina variegata* and their fraction and cisplatin at various concentrations such as 10, 20, 40, 80, 160 µg/mL.

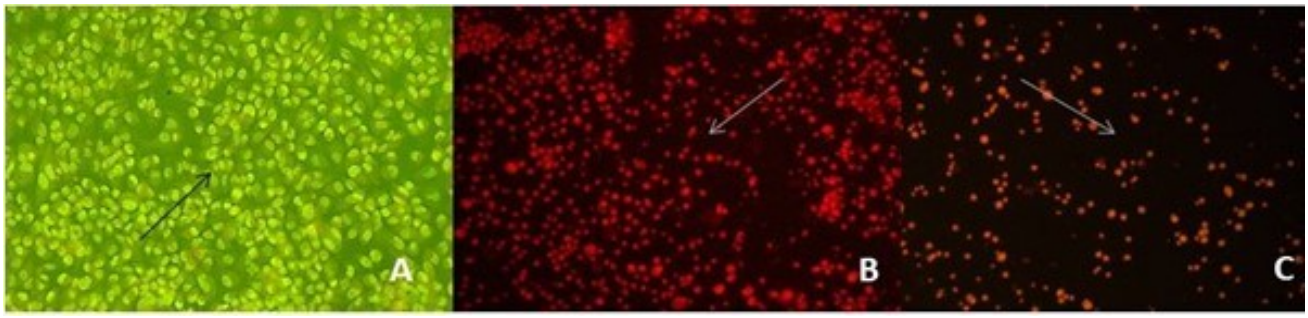


**Fig. 2.** Morphological changes of MDA-MB-231 cells by acridine orange-ethidium bromide staining, 20X. A- control cells; B- Cells treated with cisplatin at $IC_{50}$ concentration; C- cells treated with chloroform fraction of *Erythrina variegata* at $IC_{50}$ concentration. [A- normal cells with green fluorescence, B&C- have red fluorescence indicating late apoptotic cells].

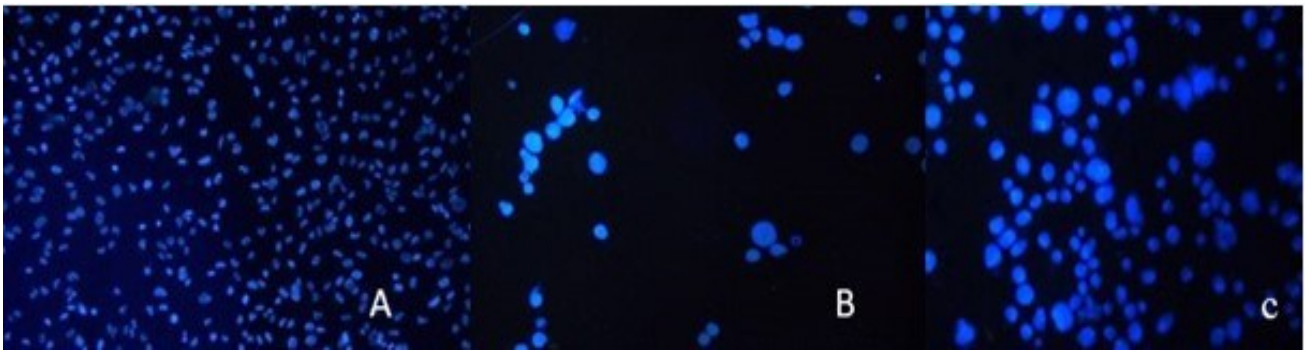


**Fig. 3.** Nuclear changes of MDA-MB-231 cells by DAPI staining, 20X. A- control cells; B- Cells treated with cisplatin at $IC_{50}$ concentration; C- cells treated with chloroform fraction of *Erythrina variegata* at $IC_{50}$ concentration. [A- normal cells with blue fluorescence, B&C- have bright blue fluorescence indicating nuclear fragmentation].

**Table 3**. Relative gene expression of *Bcl-2* in response to treatments

| Treatment | Mean $C_T$ value of GADPH | Mean $C_T$ value of Bcl-2 | $\Delta C_T$ | $\Delta\Delta C_T$ | Fold change in expression |
|---|---|---|---|---|---|
| Control | 24.61±0.04 | 26.4±0.0115 | $2.95^{c}$±0.019 | 0 | 1 |
| CFEV $IC_{50}$ | 24.453±0.4 | 27.93±0.026 | $4.69^{a}$±0.03 | 1.746667 | 0.29 |
| Cisplatin $IC_{50}$ | 26.69±0.02 | 27.16±0.023 | $4.15^{b}$±0.075 | 1.206667 | 0.433 |

*Values expressed as mean ± SEM with n=3, means bearing different superscript within each column differ significantly at $p<0.05$.

**Table 4.** Qualitative phytochemical analysis of chloroform fractions of *Erythrina variegata* (CFEV)

| Sl. No. | Phytochemical screened | Screening test | Result obtained |
|---|---|---|---|
| 1 | Steroids | Salkowski's test | + |
| | | Dragendroff's test | + |
| 2 | Alkaloids | Mayer' test | + |
| | | Wagner's test | + |
| | | Hagner's test | + |
| 3 | Glycoside | Barford's test | - |
| 4 | Phenolic compounds | Ferric chloride test | + |
| 5 | Tannins | Ferric chloride test | + |
| | | Gelatin test | + |
| 6 | Flavonoids | Ferric chloride test | + |
| | | Lead acetate test | + |
| 7 | Diterpenes | Copper acetate test | + |
| 8 | Triterpenes | Salkowski's test | + |
| 9 | Saponins | Froth test | - |

*+ indicates presence; - indicates absence.

fraction with a 0.29-fold change in expression when compared with the control. Hence, it could be concluded that *Bcl-2* gene expression was downregulated in the cell lines after treatment with the chloroform fraction.

The quantitative analysis of CFEV confirmed the presence of steroids, phenols, alkaloids, flavonoids, diterpenes, triterpenes and saponins and the result were depicted in Table 4.

Phytocompounds obtained on GC-MS analysis of CFEV are listed in Table 5 and the chromatogram was depicted in Fig. 4. The chloroform fraction of E. variegata on GC-MS analysis, revealed the presence of the following compounds: alpha-cubebene, (1r,2s,6s,7s,8s) -8-isopropyl-1-methyl-3-methylenetricyclo [4.4.0.02,7] decane-rel, gamma-muurolene, naphthalene, 1,2,3,4,4a,5,6,8a-octahydro-7-methyl-4-methylene-1-(1-methylethyl), cis- calamenene, (3s,3ar,3br,4s,7r,7ar) -4-isopropyl-3,7 dimethyloctahydro-1h-cyclopenta (1,3)cyclopropa(1,2)benzen-3-ol, 1h-cycloprop[e]azulen-7-ol, decahydro- 1,1,7-trimethyl-4-methylene-, [1ar-(1aalpha, 4aalpha,7beta,7abeta,7balpha)], neophytadiene, n-hexadecanoic acid, (1z,7r,8r)-7-methyl-4-propan-2-ylidenebicyclo[5.3.1] undec-1-en-8-ol, phytol, methyl stearate, 1-[(1s,3ar,4r,7s,7as)-4-hydroxy-4-methyl-7-propan-2-yl-1,2,3,3a,5,6,7,7a-octahydroinden-1-yl]ethenone, hexadecanoic acid, methyl ester, docosanal, 9,12-octadecadienoic acid (z,z)-, methyl ester, dotriacontanal, 1-heptacosanol, octacosanol, alpinumisoflavone, campesterol and stigmasterol. These compounds broadly come under the classification of alkaloids, diterpenes, triterpenes, fatty acid analogues and sterols.

The phytoconstituents obtained on HRLC-MS analysis are presented in Table 6 and the chromatogram was depicted in Fig. 5. The phytoconstituents obtained are malvaic acid, egallic acid, dimethyl gallic acid, cimifugin, 1-(3,4-Dihydroxyphenyl)-7-(4-hydroxy -3-methoxyphenyl)-1,6-heptadiene-3,5-dione, isoamericanol A, alpha licanic acid, gibberellin A60, gibberellin A95, kaempferol, genestein, butin, catechin, niazirinin, 8-c galactosylluteolin, 5 hydroxy 3 methoxysativan, 3, 3'-Dihydroxy-4',5,7-trimethoxyflavan, 2, 3 dihydroxy-p-cumate, melochinone, zanthodioline, dihydrocapsaicin, muricinine, alamarine, riddelliine, sesamin, fargesin, mytiltin A, visnadin, vermiol A and 3'-Hydroxy-3,4,5,4'-

**Table 5.** Gas chromatography–mass spectrometric (GC-MS) analysis of chloroform fractions of *Erythrina variegata* (CFEV)–phytocompounds obtained with retention time (min), peak area (%) and height (%)

| Sl. No. | Phytocompound | Class of compound | Retention time (%) | Peak area (%) | Height (%) |
|---|---|---|---|---|---|
| 1 | Alpha-Cubebene | Terpenes | 10.865 | 0.10 | 0.18 |
| 2 | (1R,2S,6S,7S,8S)-8-Isopropyl-1-methyl-3-methylenetricyclo [4.4.0.02,7]decane-rel | Sesquiterpene | 12.430 | 0.23 | 0.42 |
| 3 | Gamma-Muurolene | Sesquiterpene | 13.210 | 0.47 | 0.87 |
| 4 | (3S,3aR,3bR,4S,7R,7aR)-4-Isopropyl-3,7-dimethyloctahydro-1H-cyclopenta(1,3)cyclopropa(1,2)benzen-3-ol | Sesquiterpene | 13.598 | 0.67 | 0.8 |
| 5 | Naphthalene, 1,2,3,4,4a,5,6,8a-octahydro-7-methyl-4-methylene-1-(1-methylethyl) | Sesquiterpene | 13.897 | 0.56 | 1.05 |
| 6 | Cis-Calamenene | Sesquiterpene | 14.021 | 0.21 | 0.48 |
| 7 | 1H-Cycloprop[e]azulen-7-ol, decahydro-1,1,7-trimethyl-4-methylene-,[1ar(1aalpha,4aalpha,7beta,7abeta,7balpha)]- | Sesquiterpene | 15.02 | 0.53 | 0.81 |
| 8 | (1Z,7R,8R)-7-methyl-4-propan-2-ylidenebicyclo[5.3.1]undec-1-en-8-ol | Sesquiterpene | 16.892 | 0.62 | 0.97 |
| 9 | 1-[(1S,3aR,4R,7S,7aS)-4-hydroxy-4-methyl-7-propan-2-yl-1,2,3,3a,5,6,7,7a-octahydroinden-1-yl]ethanone | Sesquiterpene | 17.563 | 0.78 | 0.98 |
| 10 | Neophytadiene | Diterpenes | 18.997 | 0.34 | 0.59 |
| 11 | Hexadecanoic acid, methyl ester | Ester | 20.278 | 0.82 | 1.42 |
| 12 | 9,12-Octadecadienoic acid (Z,Z)-, methyl ester | Ester | 22.598 | 0.42 | 0.82 |
| 13 | n-Hexadecanoic acid | Fatty acid | 20.801 | 0.63 | 0.91 |
| 14 | Phytol | Diterpenes | 22.834 | 0.48 | 0.72 |
| 15 | Methyl stearate | Ester | 23.037 | 0.28 | 0.54 |
| 16 | Docosanal | Fatty alcohol | 26.825 | 0.43 | 0.73 |
| 17 | Dotriacontanal | Fatty aldehyde | 28.078 | 0.19 | 0.37 |
| 18 | 1-Heptacosanol | Fatty alcohol | 32.729 | 2.09 | 2.49 |
| 19 | Octacosanol | Fatty alcohol | 36.213 | 4.97 | 3.19 |
| 20 | Alpinumisoflavone | Alkaloid | 38.319 | 16.9 | 9.98 |
| 21 | Campesterol | Sterol | 38.884 | 3.30 | 1.79 |

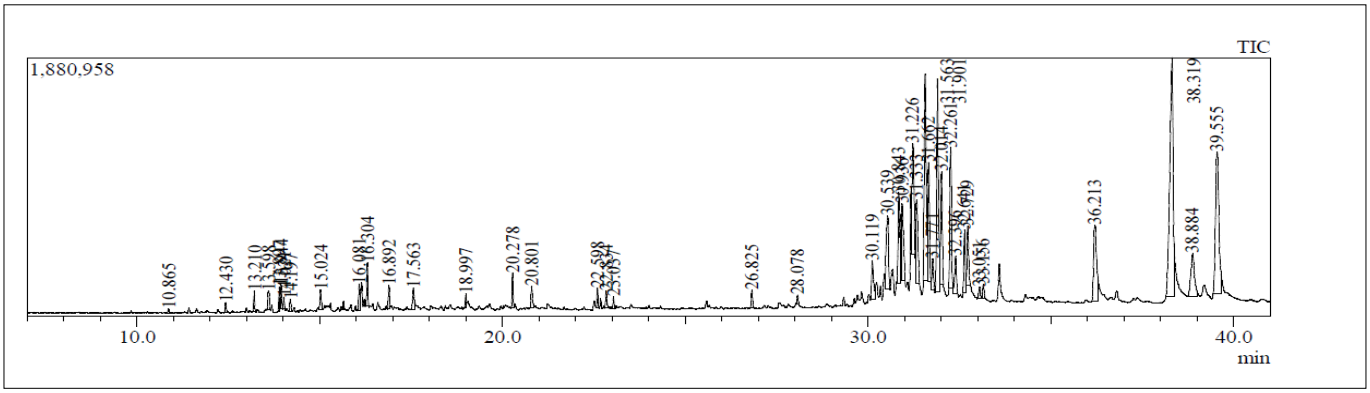


**Fig. 4.** Chromatogram of chloroform fractions of *Erythrina variegata* (CFEV) obtained using gas chromatography–mass spectrometric (GC-MS).

**Table 6.** High-resolution liquid chromatography mass spectrometry (HR-LCMS) analysis of chloroform fractions of *Erythrina variegata* (CFEV)–phytocompounds obtained with retention time (min), abundance

| Sl. No. | Phytocompounds | Class of compound | Abundance | Retention time (min) |
|---|---|---|---|---|
| 1 | Malvaic acid | Fatty acid | 735 | 20.675 |
| 2 | Egallic acid | Phenol | 789 | 7.739 |
| 3 | Dimethyl gallic acid | Phenol | 909 | 4.342 |
| 4 | Kaempferol | Flavonoid | 1262 | 7.961 |
| 5 | αlicanic acid | Triterpenes | 1382 | 17.621 |
| 6 | Gallic acid | Phenol | 1744 | 25.529 |
| 7 | Genistein | Flavonoid | 1897 | 7.462 |
| 8 | Arbutin | Glycoside | 2158 | 6.066 |
| 9 | Butin | Flavonoid | 3313 | 10.09 |
| 10 | 2,3 dihydroxy p cumate | Monoterpenes | 3826 | 10.446 |
| 11 | Catechin | Flavonoid | 12757 | 5.487 |
| 12 | Cimifugin | Phenol | 44304 | 14.3058 |
| 13 | Niazirinin | Flavonoid | 53908 | 7.264 |
| 14 | Melochinone | Alkaloid | 53932 | 5.521 |
| 15 | 1-(3,4-Dihydroxyphenyl)-7-(4-hydroxy-3-methoxyphenyl)-1,6-heptadiene-3,5-dione | Phenol | 58512 | 12.582 |
| 16 | 3'-Hydroxy-3,4,5,4'-tetramethoxystilbene | Stilbene | 66106 | 12.555 |
| 17 | 8-C-Galactosylluteolin | Flavanoid | 67892 | 8.621 |
| 18 | Zanthodioline | Alkaloid | 69048 | 9.206 |
| 19 | Dihydrocapsaicin | Alkaloid | 79478 | 10.29 |
| 20 | Fargesin | Ligan | 83967 | 11.564 |
| 21 | Muricinine | Alkaloid | 90115 | 9.965 |
| 22 | Alamarine | Alkaloid | 102328 | 16.341 |
| 23 | 5 hydroxy 3 methoxysativan | Flavonoid | 126194 | 14.071 |
| 24 | Riddelliine | Alkaloid | 152160 | 4.132 |
| 25 | Gibberellin A60 | Terpenes | 172977 | 9.458 |
| 26 | Visnadin | Pyranocoumarin | 220617 | 9.544 |
| 27 | Gibberellin A95 | Terpenes | 231883 | 12.372 |
| 28 | Isoamericanol A | Phenol | 234635 | 14.062 |
| 29 | 3,3'-Dihydroxy-4',5,7-trimethoxyflavan | Flavonoid | 344738 | 13.707 |
| 30 | Vermiol A | Phenolic acid | 1026903 | 16.483 |
| 31 | Mytilin A | Coumarin | 1366252 | 13.403 |
| 32 | Sesamin | Ligan | 3312689 | 13.907 |

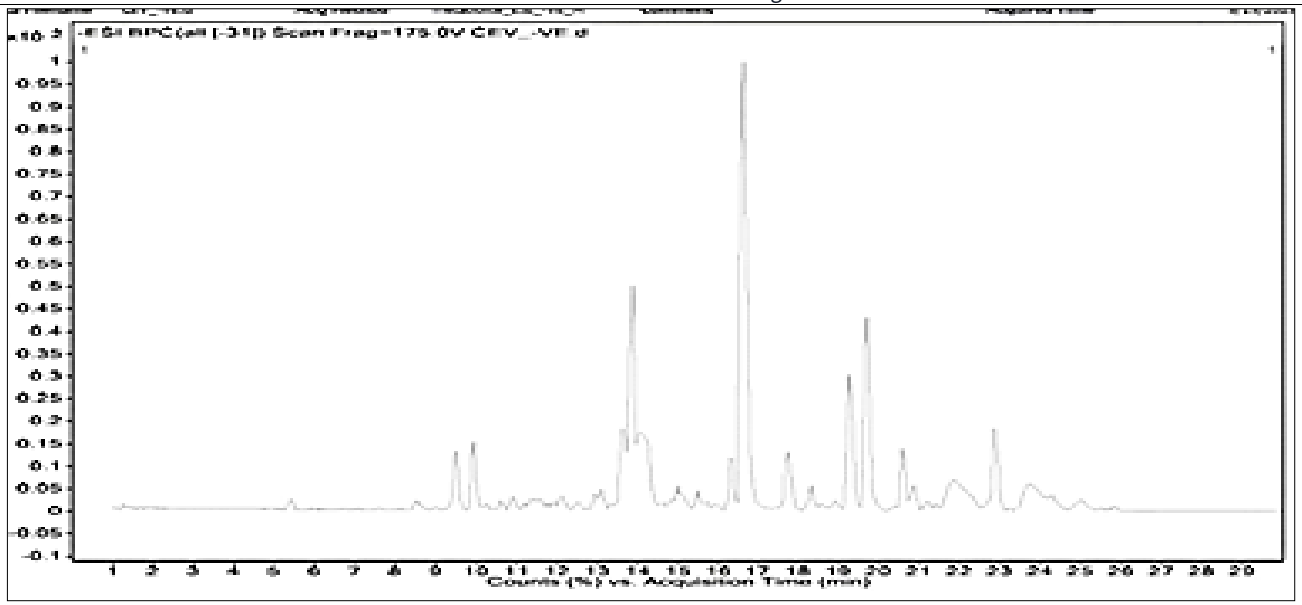

**Fig. 5.** Chromatogram of chloroform fractions of *Erythrina variegata* (CFEV) obtained using high-resolution liquid chromatography mass spectrometry (HRLC-MS).

tetramethoxystilbene. These compounds broadly come under the classification of fatty acids, phenols, flavonoids, terpenes, glycosides, stilbenes, lignans, alkaloids and coumarin derivatives.

Table 7 represents the list of 21 compounds obtained from GC–MS and 32 compounds obtained from HRLC-MS with anti-carcinogenic properties and a drug-likeness report was generated using SwissADME analysis. The standard drug, doxorubicin and the anti-cancerous phytocompounds of *E. variegata* listed in Table 7 were docked with the antiapoptotic gene BCL-2. Molecular docking analysis revealed that alpinumisoflavone and melochinone have the same binding affinity scores as that of the standard drug , while compared to the rest of the anti-carcinogenic compounds and they were ranked based on their individual binding scores (Table 8). The results of docking were depicted in Fig. 6a and Fig. 6b. Whereas certain phytocompounds that have higher binding energy when comparing to the standard drug doxorubicin but exhibited good hydrogen bonding with *Bcl-2* proteins. This suggests that those compounds whose docking score is higher than doxorubicin with highest hydrogen bond can also be a potent cytotoxic agent in this plant fraction.

**Table 7.** Compounds of gas chromatography–mass spectrometric (GC-MS) and high-resolution liquid chromatography mass spectrometry (HRLC-MS) analysis of chloroform fractions of *Erythrina variegata* (CFEV) assessed for violation of Lipinski's rule of five

| Sl. No. | Phytocomound | Lipinski's rule violation |
|---|---|---|
| | **GC-MS** | |
| 1 | Alpha-Cubebene | 1 violation |
| 2 | (1R,2S,6S,7S,8S)-8-Isopropyl-1-methyl-3-methylenetricyclo[4.4.0.02,7]decane-rel | 1 violation |
| 3 | Gamma-Muurolene | 0 violation |
| 4 | (3S,3aR,3bR,4S,7R,7aR)-4-Isopropyl-3,7-dimethyloctahydro-1H-cyclopenta(1,3)cyclopropa (1,2)benzen-3-ol | 1 violation |
| 5 | Naphthalene, 1,2,3,4,4a,5,6,8a-octahydro-7-methyl-4-methylene-1-(1-methylethyl) | 1 violation |
| 6 | Cis-Calamenene | 0 violation |
| 7 | 1H-Cycloprop[e]azulen-7-ol, decahydro-1,1,7-trimethyl-4-methylene-,[1ar (1aalpha,4aalpha,7beta,7abeta,7balpha)]- | 0 violation |
| 8 | (1Z,7R,8R)-7-methyl-4-propan-2-ylidenebicyclo[5.3.1]undec-1-en-8-ol | 0 violation |
| 9 | 1-[(1S,3aR,4R,7S,7aS)-4-hydroxy-4-methyl-7-propan-2-yl-1,2,3,3a,5,6,7,7a-octahydroinden-1-yl]ethenone | 1 violation |
| 10 | Neophytadiene | 1 violation |
| 11 | 9,12-Octadecadienoic acid (Z,Z)-, methyl ester | 1 violation |
| 12 | n-Hexadecanoic acid | 1 violation |
| 13 | Phytol | 1 violation |
| 14 | Methyl stearate | 1 violation |
| 15 | Docosanal | 1 violation |
| 16 | Dotriacontanal | 1 violation |
| 17 | 1-Heptacosanol | 1 violation |
| 18 | Octacosanol | 0 violation |
| 19 | Alpinumisoflavone | 1 violation |
| 20 | Campesterol | 1 violation |
| 21 | Stigmasterol | 1 violation |
| | **HRLC-MS** | |
| 22 | Malvaic acid | 1, violation |
| 23 | Egallic acid | 0, violation |
| 24 | Dimethyl gallic acid | 0, violation |
| 25 | Kaempferol | 0, violation |
| 26 | αlicanic acid | 0, violation |
| 27 | Gallic acid | 0, violation |
| 28 | Genistein | 0, violation |
| 29 | Arbutin | 0, violation |
| 30 | Butin | 0, violation |
| 31 | 2,3 dihydroxy p cumate | 0, violation |
| 32 | Catechin | 0, violation |
| 33 | Cimifugin | 0, violation |
| 34 | Niazirinin | 0, violation |
| 35 | Melochinone | 0, violation |
| 36 | 1-(3,4-Dihydroxyphenyl)-7-(4-hydroxy-3-methoxyphenyl)-1,6-heptadiene-3,5-dione | 0, violation |
| 37 | 3'-Hydroxy-3,4,5,4'-tetramethoxystilbene | 0, violation |
| 38 | 8-C-Galactosylluteolin | 2, violation |
| 39 | Zanthodioline | 0, violation |
| 40 | Dihydrocapsaicin | 0, violation |
| 41 | Fargesin | 0, violation |
| 42 | Muricinine | 0, violation |
| 43 | Alamarine | 0, violation |
| 44 | 5 hydroxy 3 methoxysativan | 0, violation |
| 45 | Riddelliine | 0, violation |
| 46 | Gibberellin A60 | 0, violation |
| 47 | Visnadin | 0, violation |
| 48 | Gibberellin A95 | 0, violatiom |
| 49 | Isoamericanol A | 0, violation |
| 50 | 3,3'-Dihydroxy-4',5,7-trimethoxyflavan | 0, violation |
| 51 | Vermiol A | 0, violation |
| 52 | Mytilin A | 0, violation |
| 53 | Sesamin | 0, violation |

**Table 8**. Binding energy, number and type of amino acids involved in hydrogen (H) bonds of standard drug, doxorubicin and phytoconstituents of *Erythrina variegata* obtained in gas chromatography–mass spectrometric (GC-MS) and high-resolution liquid chromatography mass spectrometry (HRLC-MS) analysis against *Bcl-2* protein

| Sl. No. | Phytocompound | Binding energy (Kcal/mol) | No. of H bonds | Amino acids involved in H bond |
|---|---|---|---|---|
| 1 | Doxorubicin | -8.4 | 0 | - |
| | **GC-MS** | | | |
| 2 | Alpinumisoflavone | -8.3 | 0 | - |
| 3 | Stigmasterol | -7.5 | 1 | GLU 133 |
| 4 | Campesterol | -7.2 | 0 | - |
| 5 | 1H-Cycloprop[e]azulen-7-ol, decahydro-1,1,7-trimethyl-4-methylene,[1ar(1aalpha,4aalpha,7beta,7abeta,7balpha)]- | -6.9 | 0 | - |
| 6 | (1z, 7r, 8r)- 7methyl-4-propan-2-yildenebicyclo(5.3.1) undec1en8-ol | -6.8 | 0 | - |
| 7 | 1-[(1S,3aR,4R,7S,7aS)-4-hydroxy-4-methyl-7-propan-2-yl-1,2,3,3a,5,6,7,7a-octahydroinden-1-yl]ethanone | -6.7 | 0 | - |
| 8 | Phytol | -6.2 | 0 | - |
| 9 | neophytadine | -6.1 | 0 | - |
| 10 | n hexadecenoic acid | -5.4 | 0 | - |
| 11 | 9,12 octadecanoic acid, methyl ester | -5.3 | 4 | ALA 97, TYR 199, ARG 143,TYR 105 |
| | **HRLC-MS** | | | |
| 12 | Melochinone | -8.4 | 2 | SER 102, GLU149 |
| 13 | Sesamin | -7.9 | 1 | ASP 108 |
| 14 | Alarmarin | -7.8 | 0 | - |
| 15 | 8-c galactosylluteolin | -7.7 | 2 | ARG 143, ASN 140 |
| 16 | Isoamericanol A | -7.7 | 1 | ARG 143 |
| 17 | 1-(3,4) dihydroxyphenyl-7-(4-hydroxy-3-methoxyphenyl 1,6 heptadiene-3,5-dione | -7.6 | 0 | - |
| 18 | 5 hydroxy 3 methoxysativan | -7.3 | 2 | ASP 108, ARG143 |
| 19 | Genestin | -7.3 | 1 | ASP 108 |
| 20 | Catechin | -7.1 | 1 | TRP 199 |
| 21 | Zantholidine | -7.1 | 1 | ALA 146 |
| 22 | Muricinine | -7 | 4 | ASP 108, LEU 134, GLU 133, ARG 143 |
| 23 | Visnadin | -6.9 | 2 | ARG143, LEU 134 |
| 24 | Riddelliine | -6.9 | 1 | ALA 97 |
| 25 | Verimol A | -6.9 | 2 | ALA 128, TR`P 173 |
| 26 | Fargesin | -6.7 | 1 | LEU 134 |
| 27 | 3,3 dihydroxy 4,5,8 trimethoxy-6,7- flavan | -6.7 | 1 | ARG 143 |
| 28 | 3 hydroxy 3,4,5,4 tetramethoxtstilbene | -6.7 | 2 | ARG 143, SER 102 |
| 29 | Niazirinin | -6.3 | 1 | VAL 130 |
| 30 | Mytilin A | -6.22 | 2 | ARG 143, ASP 137 |
| 31 | 2,3 dihydroxy-p-cumate | -6.2 | 3 | ARG143, ASP108, ALA 146 |
| 32 | Dihydrocapsain | -6.1 | 0 | - |
| 33 | s- edulinine | -6.9 | 1 | TYR 105 |
| 34 | Kaempferol | -7.1 | 2 | GLN23. SER102 |
| 35 | Alpha licanic acid | -5.7 | 1 | ASP 100 |
| 36 | Gallic acid | -6 | 5 | ARG 4, GLY6, TYR7, HIS 183, ASN 177 |
| 37 | Arbutin | -6.2 | | |
| 38 | Cimifugin | -6.9 | 1 | TYR 199 |

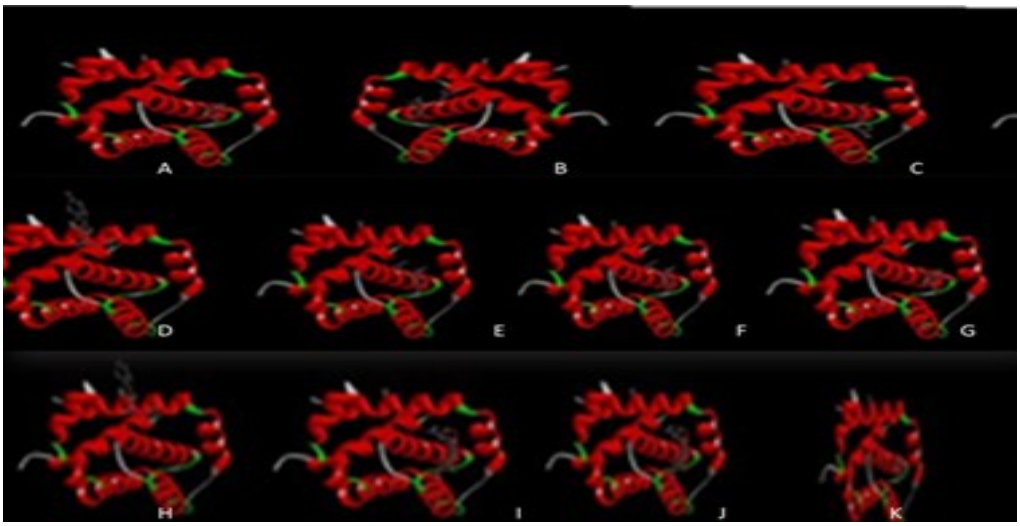


**Fig. 6a.** 3-D docked image of doxorubicin and phytoconstituents of *Erythrina variegata* in gas chromatography–mass spectrometric (GC-MS) analysis. (A. Doxorubicin, B. Alpinumisoflavone, C. Stigmasterol, D. Campesterol, E. 1H-Cycloprop\[e]azulen-7-ol, decahydro-1,1,7-trimethyl-4-methylene-\[1a (1aalpha,4aalpha,7beta,7abeta,7balpha)]-, F. (1z, 7r, 8r)-7-methyl-4-propan-2-yldenebicyclo(5.3.1)undec-1-en-8-ol, G. 1-\[(1S,3aR,4R,7S,7aS)-4-hydroxy-4-methyl-7-propan-2-yl-1,2,3,3a,5,6,7,7a-octahydroinden-1-yl]ethanone, H. Phytol, I. Neophytadine, J. n-Hexadecenoic acid, K. 9,12-octadecanoic acid and methyl ester.

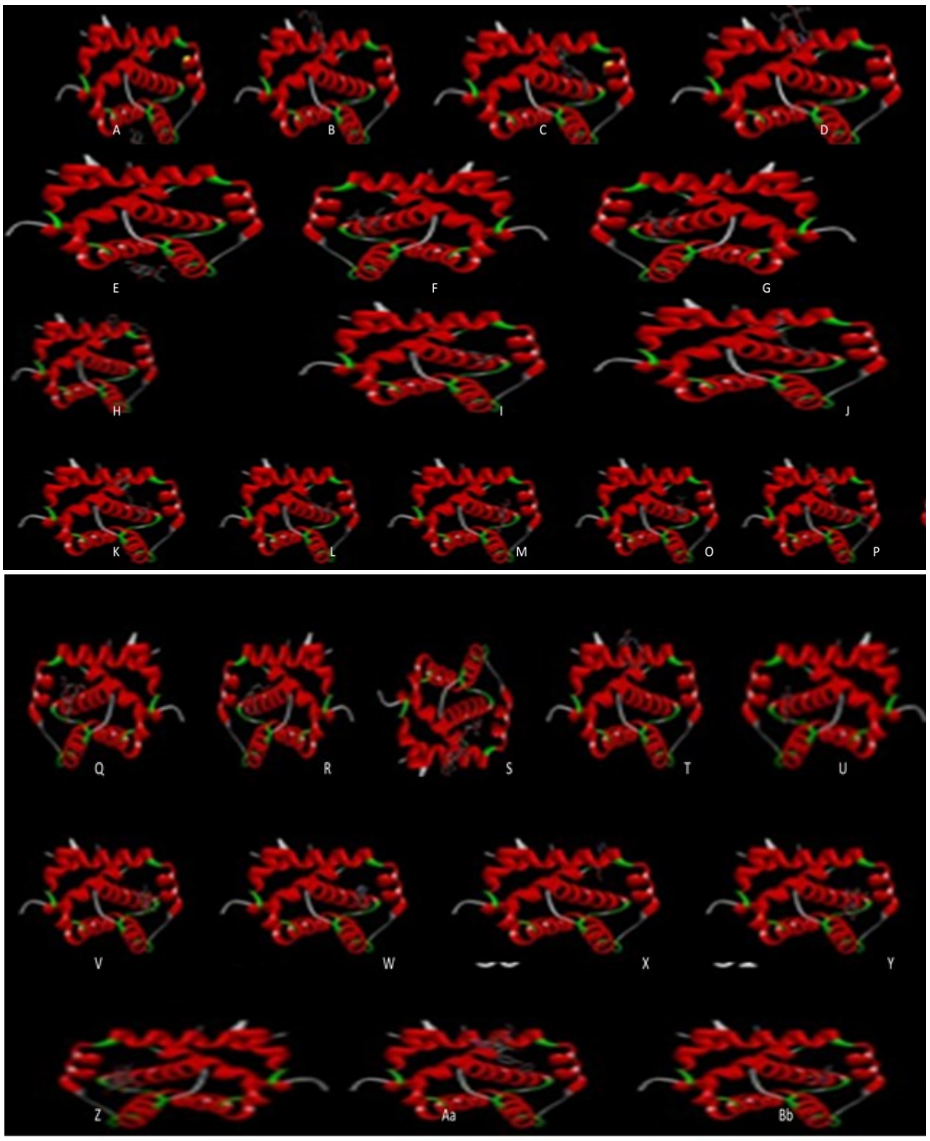


**Fig. 6b.** 3-D docked image of phytoconstituents of *Erythrina variegata* obtained from high-resolution liquid chromatography mass spectrometry (HRLC-MS) analysis (A. Melochinone, B. Sesamin, C. Alarmarin, D. 8-C-Galactosylluteolin, E. Isoamericanol A, F. 1-(3,4)-dihydroxyphenyl-7-(4-hydroxy-3-methoxyphenyl)-1,6-heptadiene-3,5-dione, G. 5-Hydroxy-3-methoxysativan, H. Genestin, I. Catechin, J. Zantholidine, K. Muricinine, L. Visnadin, M. Riddelliine, O. Verimol A, P. Fargesin, Q. 3,3-Dihydroxy-4,5,8-trimethoxy-6,7-flavan, R. 3-Hydroxy-3,4,5,4-tetramethoxystilbene, S. Niazirinin, T. Mytilin A, V. 2,3-Dihydroxy-p-cumate, 33. Dihydrocapsain, U. 7-O-(4-hydroxycinnamoyl) astragalin, W. S-edulinine, X. Kaempferol, Y. Alpha licanic acid, Z. Gallic acid, Aa. Arbutin and Bb. Cimifugin.

## Discussion

The plant material, *E. variegata,* was authenticated by nucleotide sequencing of the chloroplast ribulose 1,5-bisphosphate carboxylase (*rbcL*) gene. The sequences showed 99 % and 99.6 % similarity for the forward and reverse sequences respectively. These results are in close agreement with the *rbcL* nucleotide sequence reported earlier (15), thereby confirming accurate species authentication. The crude methanolic extract yielded 5 % from the initial dried bark and subsequent solvent partitioning generated fractions of varying polarity, enabling the enrichment of bioactive constituents.

Breast carcinoma is one of the most diagnosed malignancies worldwide and remains a leading cause of cancer-related mortality. Depending on the presence or absence of oestrogen and progesterone receptors, breast cancers are broadly classified into hormone-responsive and nonresponsive types. Triple-negative breast cancers (TNBC), which lack these receptors, are typically more invasive, aggressive and clinically challenging, necessitating the development of novel therapeutic agents effective across different breast cancer subtypes. Although earlier studies have established that the methanolic extract of *E. variegata* possesses anticancer activity (16), the specific polarity-based fractions and phytochemical groups responsible for this cytotoxicity had not yet been identified. This gap highlighted the need for further investigation. In the present study, by evaluating the cytotoxic effects of both the crude methanol extract and its solvent-partitioned fractions, the fraction containing the most potent cytotoxic constituents against TNBC cells was identified and thus provides valuable insight into the active compounds contributing to the plant's anticancer potential.

*In vitro* cytotoxic activity of the methanol extract of *E. variegata* (MEV) and its solvent-partitioned fractions was assessed using the MTT assay, which quantifies the reduction of MTT to formazan by viable cells. In accordance with NCI criteria, samples exhibiting $IC_{50}$ values below 30 µg/mL are classified as strongly cytotoxic (17). All tested samples demonstrated marked cytotoxicity against MDA-MB-231 cells, with $IC_{50}$ values falling within this threshold. Among them, the chloroform fraction (CFEV) showed the greatest potency, recording an $IC_{50}$ of 19.01 ± 1.37 µg/mL and outperforming both the

crude extract and the remaining polarity-based fractions. These observations are consistent with previous studies on *Erythrina* species, in which dichloroform fractions exhibited the highest activity against cancer cell lines such as HeLa and MCF-7 (18). Henceforth, CFEV could be chosen and scrutinized further as a potential antitumour material (19).

The MTT assay is incapacitated to detect the mode of inhibition of cell growth. Therefore, morphological staining assays were employed to confirm the mechanism of CFEV-induced cell death. Drugs frequently eliminate cancer cells through apoptosis, where apoptotic levels are positively regulated according to cellular sensitivity (20). Apoptosis plays a pivotal role in physiological growth and development by selectively removing unwanted cells. Numerous anticancer agents activate signal transduction pathways associated with programmed cell death. Although the initiation of apoptosis by therapeutic compounds is not fully understood, the morphological and biochemical alterations, such as cellular shrinkage, nuclear fragmentation and chromatin condensation, are characterised by apoptosis (21). In the present study, apoptotic mediation of CFEV-induced cytotoxicity was assessed using AO/EB dual staining, an economical and widely used technique for detecting apoptotic cells. In AO/EB staining, a clear distinction among viable, early apoptotic, late apoptotic and necrotic cells will be observed. In the present study, AO permeated viable control cells, staining its nuclei green by binding to DNA, whereas EB stained the nuclei of treated cells to orange–red due to its affinity for fragmented DNA, indicating these cells in late apoptosis and necrosis stage. These observations were further supported by DAPI staining, which revealed nuclear fragmentation and chromatin condensation, which are the hallmarks of apoptosis. Similar apoptotic features have been described for alpinumisoflavone and other *Erythrina*-derived flavonoids, supporting the role of flavonoid-rich fractions in inducing programmed cell death (22).

At the molecular level, apoptosis induced by CFEV was further elucidated by examining the expression of the anti-apoptotic gene *Bcl-2*, a key regulator of mitochondrial outer membrane permeabilization within the intrinsic apoptotic pathway. *Bcl-2* proteins localized across the mitochondrial, endoplasmic reticulum and nuclear membranes function in maintaining mitochondrial transmembrane potential and prevent the release of apoptogenic factors such as cytochrome c. Thus, the down-regulation of the *Bcl-2* gene disrupts cellular homeostasis and facilitates caspase activation (23). The diminished *Bcl-2* expression by the cells treated with $IC_{50}$ value of CFEV suggests that the chloroform fraction triggers apoptosis via the mitochondria-dependent intrinsic pathway, which agrees with previous reports describing similar mechanisms for *Erythrina* derived metabolites such as stigmasterol, sesamin, alpinumisoflavone and melochinone (24). Collectively, the molecular profiling together with the observed nuclear morphological alterations reinforce that CFEV mediates its cytotoxicity predominantly through apoptosis. Supporting these findings, molecular docking studies demonstrated strong binding affinities of key CFEV constituents such as alpinumisoflavone (-8.4 kcal/mol), melochinone (-8.4 kcal/mol), isoamericanol A (-7.7 kcal/mol), 1-(3,4-dihydroxyphenyl)-7-(4-hydroxy-3-methoxyphenyl)-1,6-heptadiene-3,5-dione (–7.6 kcal/mol) and 5-hydroxy-3-methoxysativan (-7.3 kcal/mol) towards the *Bcl-2* protein, comparable to that of the standard chemotherapeutic agent doxorubicin (-8.4 kcal/mol). These *in silico* results are in agreement with prior studies reporting that plant-derived flavonoids, stilbenes and sterols can interact with the *Bcl-2* protein to modulate mitochondria-mediated apoptosis, further validating the apoptotic mechanism of CFEV at both molecular and computational levels (25).

Despite these promising findings, a key limitation of this study is the use of a single *in vitro* cell line model. Cell line models, represent a simplified biological system and do not fully capture the complexity, cellular heterogeneity and tissue-specific microenvironments found *in vivo*. Therefore, the observed cytotoxicity in this specific cell line may not be fully translatable to other cell types or a whole organism, necessitating further validation in more complex models or alternative cell lines (26). Subsequent investigations should therefore include testing on non-cancerous or additional cancer lines to confirm the generalizability of the results. Moreover, although *Bcl-2* suppression was confirmed, complementary markers of the intrinsic apoptotic cascade, such as Bax, cytochrome c release and caspase activation, were not evaluated. In the future there is a need to isolate and characterize key active constituents, validate their mechanisms across multiple TNBC and non-cancerous cell lines, and explore advanced drug delivery approaches for lipophilic compounds like phytol and stigmasterol that violate Lipinski's rule.

## Conclusion

The results indicated that the CFEV possessed anticancer potential *in vitro* against MDA-MB-231 cell lines. The fraction was found to induce apoptosis through intrinsic apoptotic pathway as noted with AO/EB and DAPI staining. The fraction also downregulated *Bcl-2* expression, the antiapoptotic gene, which substantiated the observed apoptosis *in vitro*. Alpinumisoflavone, melochinone, isoamericanol A, 1-(3,4-dihydroxyphenyl)-7-(4-hydroxy-3-methoxyphenyl)-1,6-heptadiene-3,5-dione and 5-hydroxy-3-methoxysativan obtained on GC-MS and HRLC-MS analysis exhibited strong binding affinity to *Bcl-2* in molecular docking studies, which could act as a contributing factor for the depicted anticancer activity *in vitro*.

## Acknowledgements

The authors are thankful to Sophisticated Analytical Instrument Facility, Indian Institute of Technology, Bombay for help in conducting HRLC-MS analysis. The analysis charge for the same was funded from the from National Medicinal Plants Board, Ministry of AYUSH, Government of India grant to the second author with grant no. F.No.Z. 18017/187/CSS/R&D/KE-02/2020-21-NMPB-IVA. The authors are also thankful to Kerala Veterinary and Animal Sciences University for providing funding as MVSc grant to first author with grant number KVASU/2023/58/MVM/ABT.

## Authors' contributions

PV contributed to writing the original draft and was responsible for visualization, validation, software, methodology, investigation, formal analysis, and data curation. BJK contributed to writing, review and editing and was responsible for validation, supervision, resources, project administration, investigation, funding acquisition, data curation and conceptualization. Both authors read and approved the final manuscript.

## Compliance with ethical standards

**Conflict of interest:** Authors do not have any conflict of interests to declare.

**Ethical issues:** None

### Declaration of generative AI and AI-assisted technologies in the writing process

During the preparation of this work, the author(s) used ChatGPT to improve language and readability. After using this tool/service, the author(s) reviewed and edited the content as needed and took full responsibility for the content of the publication.

## References


1. Giaquinto AN, Sung H, Newman LA, Freedman RA, Smith RA, Star J, et al. Breast cancer statistics 2024. CA Cancer J Clin. 2024;74(6):477–95. https://doi.org/10.3322/caac.21863
2. Kesireddy M, Elsayed L, Shostrom VK, Agarwal P, Asif S, Yellala A, et al. Overall survival and prognostic factors in metastatic triple-negative breast cancer: a national cancer database analysis. Cancers. 2024;16 (10):1791. https://doi.org/10.3390/cancers16101791
3. Li Y, Zhang H, Merkher Y, Chen L, Liu N, Leonov S, et al. Recent advances in therapeutic strategies for triple-negative breast cancer. J Hematol Oncol. 2022;15(1):121. https://doi.org/10.1186/s13045-022-01341-0
4. Cai Y, Luo Q, Sun M, Corke H. Antioxidant activity and phenolic compounds of 112 traditional Chinese medicinal plants associated with anticancer. Life Sci. 2004;74(17):2157–64. https://doi.org/10.1016/j.lfs.2003.09.047
5. Jiangsu New Medical College, editor. A dictionary of Chinese herbal medicine. Shanghai: Shanghai People's Press; 1977. p. 1941–42.
6. Sarragiotto MH, Filho HL, Marsailoi AJ. Eritrosine-N-oxide and erythartine-N-oxide, two novel alkaloids from *Erythrina mulungu*. Can J Chem. 1972;59:1272.
7. Ito K, Haruna M, Jinno V, Furukawa H. Studies on the *Erythrina* alkaloids. XI. Alkaloids of *Erythrina crystagalli* LINN. Structure of a new alkaloid, crystamidine. Chem Pharm Bull. 1976;24:52–55. https://doi.org/10.1248/cpb.24.52
8. John R, Kariyil BJ, Usha PTA, Surya S. Apoptosis mediated cytotoxic potential of *Erythrina variegata* L. stem bark in human breast carcinoma cell lines. Indian J Exp Biol. 2021;59(7):437–47.
9. Mosmann T. Rapid colorimetric assay for cellular growth and survival: application to proliferation and cytotoxicity assays. J Immunol Methods. 1983;65(1-2):55–63. https://doi.org/10.1016/0022-1759(83)90303-4
10. Ribble D, Goldstein NB, Norris DA, Shellman YG. A simple technique for quantifying apoptosis in 96-well plates. BMC Biotechnol. 2005;5:12. https://doi.org/10.1186/1472-6750-5-12
11. Livak KJ, Schmittgen TD. Analysis of relative gene expression data using real-time quantitative PCR and the 2−ΔΔCT method. Methods. 2001;25(4):402–08. https://doi.org/10.1006/meth.2001.1262
12. Harborne JB. The natural distribution in angiosperms of anthocyanins acylated with aliphatic dicarboxylic acids. Phytochemistry. 1986;25(8):1887–94. https://doi.org/10.1016/S0031-9422(00)81168-1
13. Irulandi K, Geetha S, Tamilselvan A, Mehalingam P. GC-MS analysis and phytochemical studies of methanolic fruits extract of *Garcinia cambogia* Hort ex Boerl and Ziziphus trinervia Roth. J Adv Appl Sci Res. 2016;1(3):90–95. https://doi.org/10.46947/joaasr13201623
14. Filimonov DA, Lagunin AA, Gloriozova TA, Rudik AV, Druzhilovskii DS, Pogodin PV, et al. Prediction of the biological activity spectra of organic compounds using the PASS online web resource. Chem Heterocycl Compd. 2014;50(3):444–57. https://doi.org/10.1007/s10593-014-1496-1
15. De Luca A, Sibilio G, De Luca P, Del Guacchio E. DNA barcoding to confirm the morphological identification of the coral trees *(Erythrina* spp., Fabaceae) in the ancient gardens of Naples (Campania, Italy). Plants. 2018;7(2):43. https://doi.org/10.3390/plants7020043
16. John R, Kariyil BJ, PTA U. Apoptosis mediated cytotoxic potential of *Erythrina variegata* L. stem bark in human breast carcinoma cell lines. Indian J Exp Biol. 2021;59(7):437–47.
17. Gopalakrishnan A, Kariyil BJ, John R, Usha PA. Phytochemical evaluation and cytotoxic potential of chloroform soluble fraction of methanol extract of *Thespesia populnea* in human breast cancer cell lines. Pharmacogn Mag. 2019;15(62):150–54.
18. Olawale F, Bodede O, Ariatti M, Singh M. Isolation, characterization, antioxidant and anticancer activities of compounds from *Erythrina caffra* stem bark extract. Antioxidants. 2025;14(9):1035. https://doi.org/10.3390/antiox14091035
19. Sharma D, Rawat I, Goel HC. Anticancer and anti-inflammatory activities of some dietary cucurbits. Indian J Exp Biol. 2015;53:216–21.
20. Thompson CB. Apoptosis in the pathogenesis and treatment of disease. Science. 1995;267(5203):1456–62. https://doi.org/10.1126/science.7878464
21. Hengartner MO. The biochemistry of apoptosis. Nature. 2000;407 (6805):770–76. https://doi.org/10.1038/35037710
22. AmeliMojarad M, Pourmahdian A. The inhibitory role of stigmasterol on tumor growth by inducing apoptosis in Balb/c mouse with spontaneous breast tumor (SMMT). BMC Pharmacol Toxicol. 2022;23(1):42. https://doi.org/10.1186/s40360-022-00578-2
23. Gotow T, Shibata M, Kanamori S, Tokuno O, Ohsawa Y, Sato N, et al. Selective localization of Bcl-2 to the inner mitochondrial and smooth endoplasmic reticulum membranes in mammalian cells. Cell Death Differ. 2000;7(7):666–74. https://doi.org/10.1038/sj.cdd.4400694
24. Lee W, Song G, Bae H. In vitro and in silico study of the synergistic anticancer effect of alpinumisoflavone with gemcitabine on pancreatic ductal adenocarcinoma through suppression of ribonucleotide reductase subunit-M1. Eur J Pharm Sci. 2025;204:106969. https://doi.org/10.1016/j.ejps.2024.106969
25. Piotrowska-Kempisty H, Ruciński M, Borys S, Kucińska M, Kaczmarek M, Zawierucha P, et al. 3′-Hydroxy-3,4,5,4′-tetramethoxystilbene, the metabolite of resveratrol analogue DMU-212, inhibits ovarian cancer cell growth in vitro and in a mice xenograft model. Sci Rep. 2016;6 (1):32627. https://doi.org/10.1038/srep32627
26. Horvath P, Aulner N, Bickle M, Davies AM, Nery ED, Ebner D, et al. Screening out irrelevant cell-based models of disease. Nat Rev Drug Discov. 2016;15(11):751–69. https://doi.org/10.1038/nrd.2016.175


### Additional information


**Peer review**: Publisher thanks Sectional Editor and the other anonymous reviewers for their contribution to the peer review of this work.

**Reprints & permissions information** is available at https://horizonepublishing.com/journals/index.php/PST/open_access_policy

**Publisher's Note**: Horizon e-Publishing Group remains neutral with regard to jurisdictional claims in published maps and institutional affiliations.

**Indexing**: Plant Science Today, published by Horizon e-Publishing Group, is covered by Scopus, Web of Science, BIOSIS Previews, Clarivate Analytics, NAAS, UGC Care, etc. See https://horizonepublishing.com/journals/index.php/PST/indexing_abstracting





**Publisher information:** Plant Science Today is published by HORIZON e-Publishing Group with support from Empirion Publishers Private Limited, Thiruvananthapuram, India.